

RETROFITTING OF SHEARWALLS IN DIFFERENT METHODS

H.K. Choi¹, Y.C. Choi², M.S. Lee³, L.H. Lee⁴ and C.S. Choi⁵

¹ *Ph.D Candidate, Division of Architectural Engineering, Hanyang Univ., Seoul, Korea(R)*

² *Professor, Department of Architectural Environmental Engineering and Building Service, Chungwoon Univ., Hong-Sung, Korea(R)*

³ *Postdoctoral Researcher, BK21 Architectural Engineering Program (SAPEC), Hanyang Univ., Seoul, Korea(R)*

⁴ *President, Chungwoon University, Hong-Sung, Korea(R)*

⁵ *Professor, Division of Architectural Engineering, Hanyang Univ., Seoul, Korea(R)*

Email: chk7796@naver.com, 21ycchoi@naver.com, moonlee@hanyang.ac.kr, leelh@chungwoon.ac.kr, ccs5530@hanyang.ac.kr

ABSTRACT :

The objective of this paper is to present the test results and structural behavior of perforated RC shear walls and to introduce effective retrofitting methods by evaluating efficacy of CFS, Steel plate, MDF, and ECC. A series of six wall specimens were tested. One specimen was a prototype wall without openings and five specimens had openings. Four specimens were retrofitted using CFS, Steel plate, MDF, and ECC. The specimens were 1/2-scale representations of a one-story wall in an apartment building in Korea built in the 1980s. The retrofitted specimens showed higher value of peak load, but they exhibited lower energy dissipation capacity than the prototype specimen. The test results showed that failure mechanism of specimens was governed by shear fracture and the strength of specimens was varied depending on the retrofitting strategy used.

KEYWORDS:

Retrofitting, Shearwall, CFS, Steel Plate, ECC, MDF

1. INTRODUCTION

Recently, for more demands on economical benefits and environmental conservation, many engineers prefer remodeling of existing buildings to constructing of new buildings. Remodeling is also an environmentally-friendly approach that reduces the amount of waste in construction site. However, remodeling can sometimes include partial destruction of the structural members of buildings. In the case of the remodeling of shear wall system apartment, it is necessary to make openings at the wall for horizontal expansion. Loss of wall area due to the openings causes decrease of wall capacity and this may cause collapse of the whole structures. Therefore, it is important that the structural system maintains the required lateral resistance and stiffness and performs appropriate seismic behavior after retrofitting.

There are several retrofitting methods for reinforced concrete structures. Recently many engineers prefer to use ductile material such as carbon fiber sheets (CFS), steel plate, micro defect free (MDF), and engineered cementitious composites (ECC). Retrofitting method using CFS and Steel Plate are considered easier way of retrofitting than sectional expansion retrofitting methods using ECC and MDF. However, ECC or MDF have other types of advantage. The advantage of high ductility in the hardened state and the flexible processing in the fresh state makes ECC more attractive for a broad range of applications. High performance fiber reinforced cementitious composites (HPFRCC) is a matrix material based on fiber reinforced cement, which exhibits tensile strain-hardening behavior under uniaxial tension by redistributing stresses in multiple cracks. ECC is one of the HPFRCCs that contain fiber of approximately 2% in volume. Figure 1 shows tensile strain capacity of HPFRCC over 3%, approximately 300 times larger than that of normal concrete or fiber reinforced concrete (FRC). MDF is newly developed shot concrete that is widely used for retrofitting of large structures and is renowned for its high-speed hardening.

Studies on HPFRCC have rarely been done as structural members. Previous experiments focused on the material's characteristic before and after hardened state and manufacturing skill. In this experimental program,

the focus was on the structural performance of perforated RC walls retrofitted by ECC and MDF. Four types of retrofitting method using CFS, steel plate, ECC, and MDF have the same object of increasing of the member strength. However, these four retrofitting methods showed different behaviour and different developing time of retrofitting effect. Strength degradation ratio caused by loss of wall area and effectiveness and behaviour of different retrofitting methods were investigated in this study.

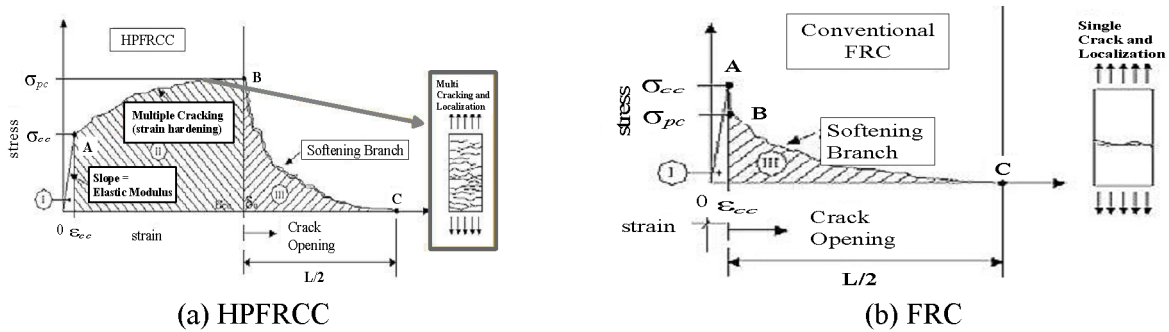


Fig 1. Pseudo strain hardening characteristics of HPFRCC

2. EXPERIMENTAL RESEARCH

2.1. Specimen Description

As shown in Table 1, a series of six wall specimens were tested. The specimens were 1/2-scale representations of a one-story wall in a Korean apartment building that was built in the 1980s. A prototype specimen (WB-Solid) represented undamaged wall which had 21MPa compressive strength of concrete and 400MPa tensile strength of reinforcement. Rest of the specimens had 900mm x 1050mm artificial openings located at the bottom center of the specimens. Four of them were retrofitted using steel plates, CFS, ECC, and MDF. Plate thickness of 3mm was chosen for WB-St. Plate. For WB-ECC and WB-MDF, ECC and MDF were cast-in-placed with a thickness of 30mm over a 10cm spacing wire mesh inserted to protect them from shrinkage and crack on both sides of the wall. Figures 2 and 3 shows size and retrofit area of specimens.

Table 1. List of Specimens

Specimen	Opening ratio	Retrofit material	Reinforcement		$l_w \times h_w \times t$ [mm]
WB-Solid	Non opening	-	Ver. D6 @255	Hor. D6 @255	3000×130×100
WB-0.23	23% (900mm×1050mm)	Without retrofit			
WB-CFS		Carbon fiber sheet			
WB-St. Plate		Steel plate			
WB-ECC		ECC			
WB-MDF		MDF			

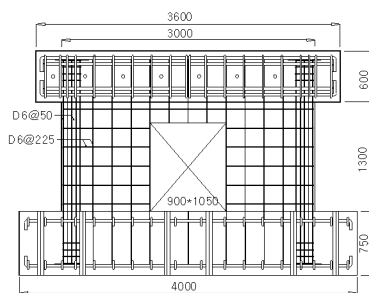


Figure 2. Specimen details

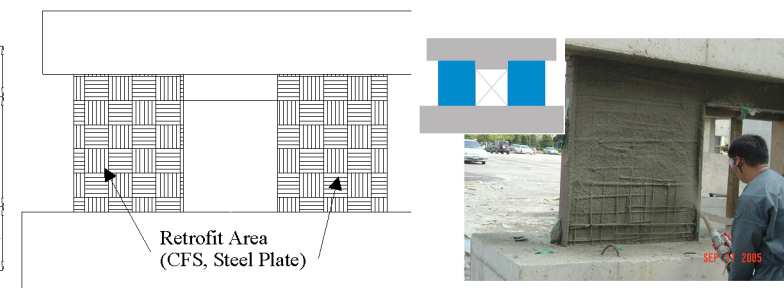


Figure 3. Retrofit Area

2.2. Test Set-up

A picture of the test setup is shown in Figure 4. Tests were conducted in the laboratory with three dimensional reaction walls. Two bars were mounted vertically to apply constant axial compression of 630kN during testing. This corresponded to approximately 10% of the computed concentric capacity of the wall. Displacement controlled lateral load was applied at the top of the wall by a 2000kN hydraulic actuator mounted between the specimen and a reaction wall. In order to prevent lateral buckling of 2nd story slabs, frames were assembled at the edge of slabs. Guide beams and ball zigs were used to minimize out-of-plane movement and simulate the diaphragm effect of a slab. Hinges were installed to simulate appropriate slab rotation. In order to measure the lateral displacement of specimens, LVDTs were mounted to the end of each floor slabs. To measure diagonal deformation of walls, which was shear deformation of walls, additional LVDTs were installed at the edge of walls and the center of walls. Displacement controlled lateral load history for the test is shown in Figure 5. Lateral drift was defined as rotational angle, which was displacement over height, of 1/1000, 1/500, 1/300, 1/250, 1/200, and applied as reversed cyclic loads. Each steps of this cyclic load repeated three times.

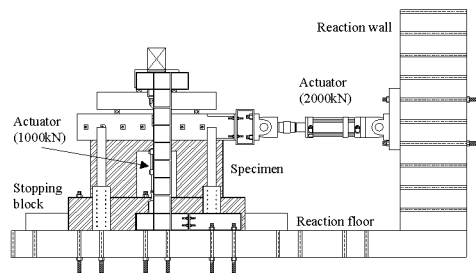


Figure 4. Test Setup

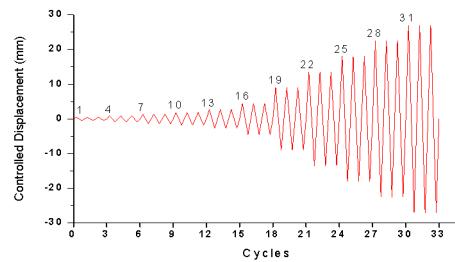


Figure 5. Loading History

3. EXPERIMENTAL RESULTS

3.1. Failure Pattern

Figure 6 illustrates the specimens' crack patterns. Each specimen showed shear failure rather than flexural failure.

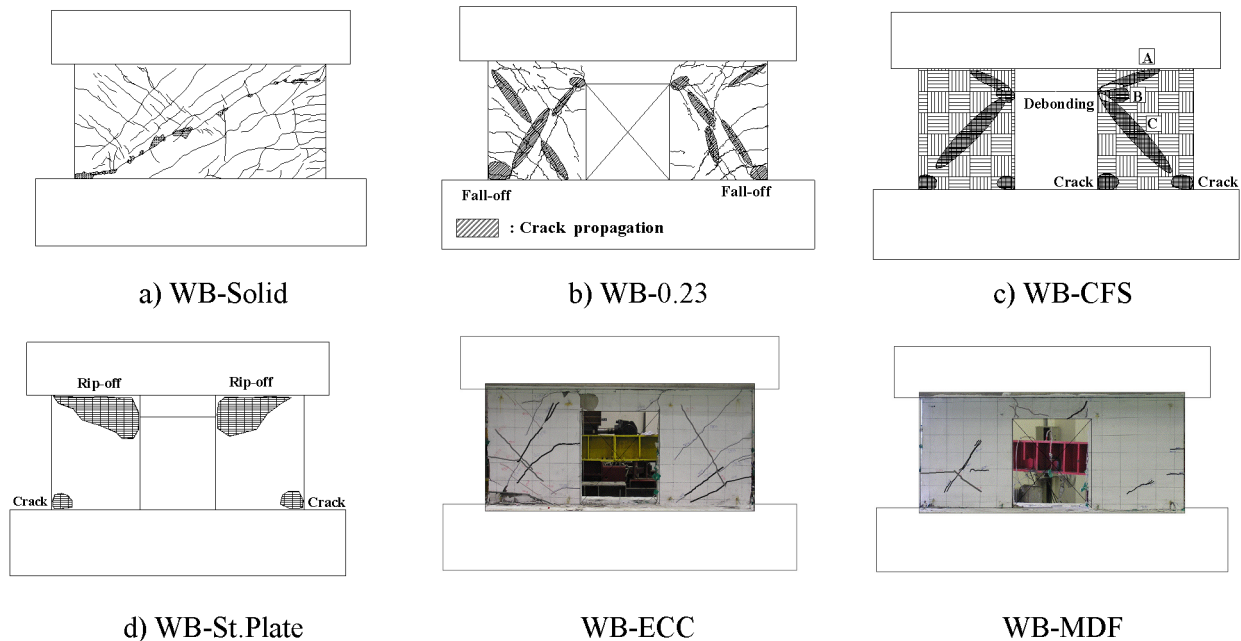


Figure 6. Crack Patterns after Failure

WB-Solid showed typical shear failure because it had a low aspect ratio. WB-0.23 showed shear failure and peeling off of the concrete surface at the opening's corners. WB-St. Plate failed by debonding of the retrofitting material. WB-CFS was also failed by debonding of retrofitting material, CFS. For WB-MDF, as cracks developed on the web and interface of the wall, MDF was separated from the wall at a drift of 0.9%, and compression failure occurred at the base. For WB-ECC, the high-tensile-fiber contained in ECC controlled cracking effectively, and cracks on the web of the wall were hardly noticeable until a drift of 0.9%. At a drift of 1%, diagonal hairline cracks occurred on the web of the wall, while cracks at the interface between ECC and the wall transferred to the wall and developed in plane direction of the wall, and then compression failure was followed at the base. The two strengthened specimens failed after crack propagation at the interface but there was a noticeable difference between them. Interface crack in WB-ECC propagated toward the wall, while interface crack in WB-MDF developed within the interface. This indicated that the ECC material attached better to the wall face than the MDF material. All retrofitted specimens showed debonding of retrofitting material from the web of the wall.

3.2. Load-Displacement Relationship

Figure 7 illustrates the specimens' load-displacement relationship. Load-displacement relationship of WB-Solid had the maximum strength of 740kN and did not show sudden degradation of stiffness and strength after the maximum strength was reached. The maximum strength of the WB-0.23 was 555kN, and it was 25% decrease of strength compared to that of WB-Solid. The maximum strength of all retrofitted specimens was larger than that of WB-Solid. The strength of WB-CFS, WB-St. Plate, WB-MDF, and WB-ECC were 13%, 12%, 20% and 6% higher than that of prototype specimen, WB-Solid, respectively.

All retrofitted specimens failed with debonding of retrofitting material. In the case of WB-CFS, peak load was measured when tilting of CFS at the wall toe and opening edge occurred. WB-St. Plate's failure time was not accurate because it was not possible to observe inside the steel plate during the test. However, WB-ECC showed higher bond capacity between ECC and the wall. Lastly, in the case of WB-MDF, by showing different strain of two materials, MDF and concrete, the lowest peak load was observed. Unlike other retrofitted methods, the strength of the wall of WB-MDF was dramatically reduced after the maximum strength. This sudden drop is mainly attributed to the absence of the ductile material that can resist fracture due to large deflection and the partial destruction of bond between the retrofitting material and concrete surface. This is clearly shown in Figure 7(f).

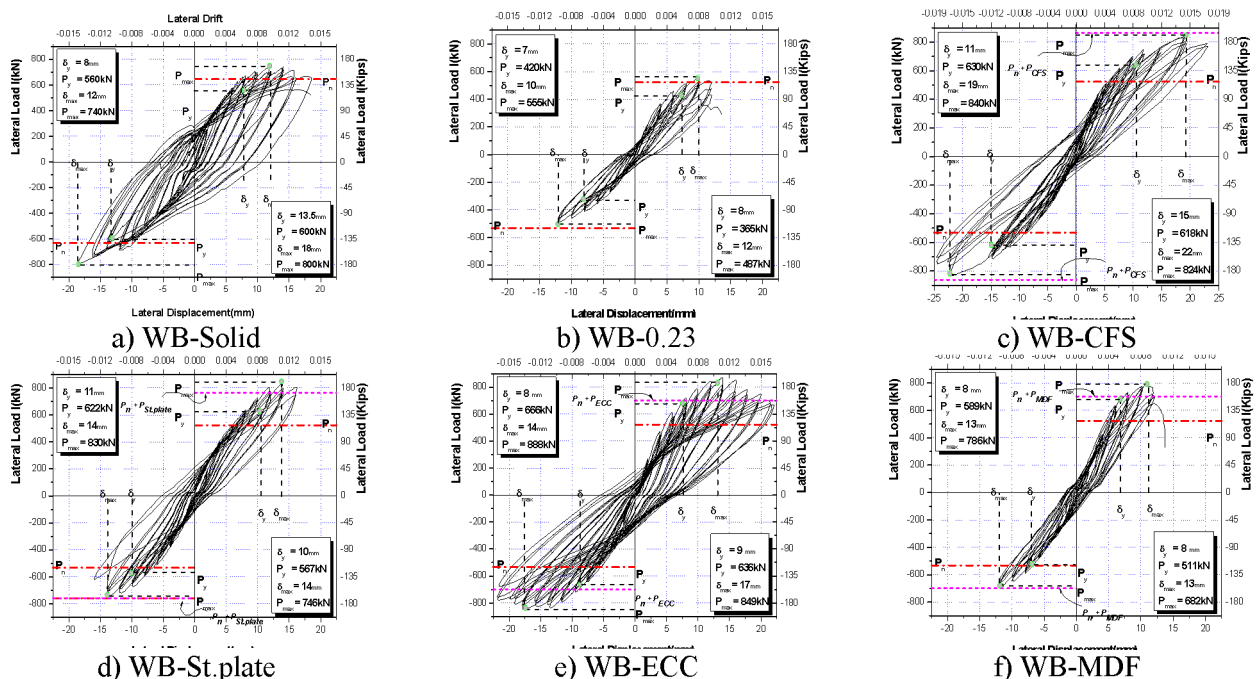


Fig. 7 Load-Displacement Relationship

Table 2. Results of the test

Specimen		P_{cr} (kN)	P_y (kN)	P_u (kN)	${}_{THE}P_u$ (kN)	$\frac{P_u}{{}_{THE}P_u}$	δ_y	δ_u	θ_y	θ_u	μ
WB-Solid	Pos	320	560	740	640	1.15	8	12	0.61	1/108	1.5
	Neg	290	600	800		1.25	13.5	18	1.03	1/71	1.3
WB-0.23	Pos	280	420	555	510	1.08	7	10	0.53	1/130	1.4
	Neg	250	365	487		0.95	8	12	0.61	1/108	1.5
WB-CFS	Pos	290	630	840	840 (325)*	1	11	19	0.84	1/68	1.7
	Neg	270	618	824		0.98	15	22	1.69	1/59	1.4
WB-St.plate	Pos	270	622	830	784 (274)*	1.05	11	14	0.84	1/92	1.2
	Neg	230	567	746		0.95	10	14	0.76	1/92	1.4
WB-ECC	Pos	260	666	888	694 (184)*	1.27	8	14	0.61	1/92	1.7
	Neg	240	636	849		1.22	9	17	0.69	1/76	1.8
WB-MDF	Pos	230	589	786	694 (184)*	1.13	8	13	0.61	1/100	1.6
	Neg	220	511	682		0.98	8.2	13	0.61	1/100	1.6

P_{cr} : initial crack load, P_y : yield load, P_u : maximum load (testing value),
 ${}_{THE}P_u$: maximum ultimate design strength (retrofit strength) * δ_y : displacement corresponding to the P_y ,
 δ_u : displacement corresponding to the P_u , θ_y : drift corresponding to the yielding, θ_u : deformation capacity,
 μ : displacement ductility ratio

3.3. Stiffness and Ductility

As shown in Figure 8, all specimens showed stiffness degradation as the load cycles increased. Specifically, by comparing non-retrofitted specimens, WB-Solid showed gentle degradation of stiffness in the beginning, but after diagonal crack occurred, stiffness of the specimen steeply decreased. In the case of retrofitted specimens, initial stiffness of the WB-CFS (111.4kN/mm), WB-St. Plate (119kN/mm), WB-MDF (118kN/mm) and WB-ECC (136kN/mm) were higher than that of WB-Solid (119kN/mm). Despite identical amount of retrofitted materials used for WB-ECC and WB-MDF, initial stiffness of the WB-ECC was 15% higher than that of WB-MDF. This can be attributed to the high tensile strength of the fiber that delays initial hairline crack. The definition of ductility ratio (μ) is a maximum displacement divided by the displacement at yield. Yield displacement is defined as displacement value from the backbone curve when the load is $0.75 P_u$. As Table 2 is shown, the ductility ratio of WB-Solid, WB-0.23, WB-CFS, WB-St. Plate, WB-ECC and WB-MDF are 1.5, 1.4, 1.7, 1.2, 1.7 and 1.6, respectively.

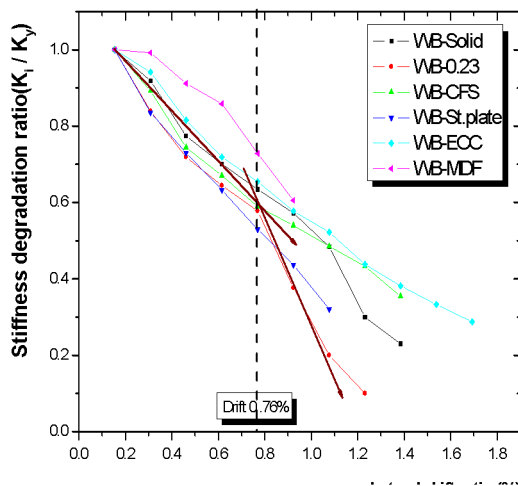


Fig 8. Stiffness and Ductility

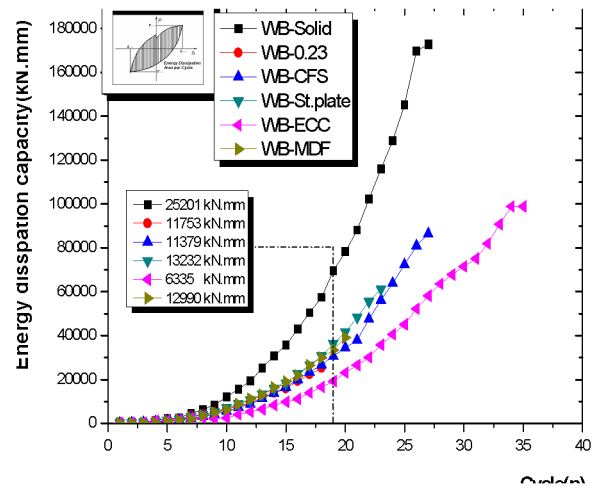


Fig 9. Energy dissipation capacity of all specimens

3.4. Energy Dissipation Characteristics

Energy dissipation capacity of specimen can be calculated by adding total enclosed area of load-displacement relation curve. Figure 9 shows comparison of energy dissipation capacity of each specimen. Energy dissipated area, which is used for damping ratio of system, of WB-Solid showed comparatively higher value than other specimens. Accumulated energy dissipation area of WB-Solid, WB-0.23, WB-CFS, WB-St. Plate, WB-ECC and WB-MDF were 25201kN • mm, 11753kN • mm, 11379kN • mm, 13232kN • mm, 6335kN • mm and 12990kN • mm, respectively at the same rotational angle of 0.92%, which was the last rotational angle of WB-0.23. By having opening of the walls, accumulative energy dissipating area decreased approximately 50%. It was thought that effective area loss of wall and damage of reinforcement caused reduction of energy dissipation capacity of the walls. Among the specimens with openings, WB-St. Plate showed the highest value of energy dissipation capacity.

3.5. Retrofitting Effect

Figure 10 and Figure 11 represent the backbone curve and design load vs. measured maximum load for all specimens. As shown in Figure 10, all retrofitting methods were valid and effective, because they showed larger capacity than WB-0.23. However, MDF retrofitting method was less effective than other retrofitting method because WB-MDF showed sudden drop of strength just after the maximum loads. Since WB-ECC showed highest ductility and shear capacity, it is thought that ECC was the most effective retrofitting method. Figure 11 shows that our design philosophy for retrofitting is slightly under estimate the strength of specimens. And we can know from this figure about retrofitting effect makes damaged specimens slightly stronger than solid specimen.

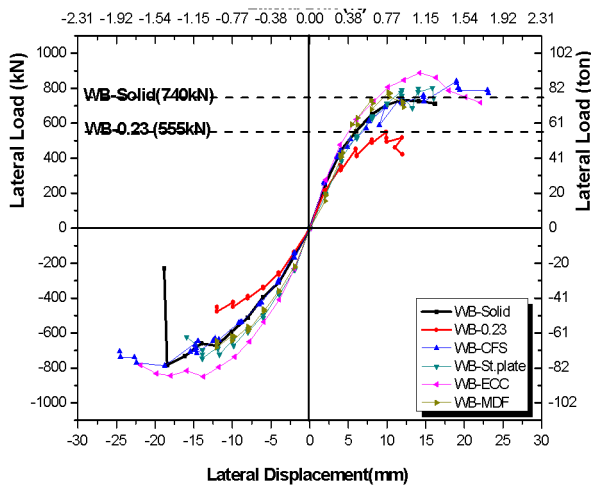


Figure 10. Back-bone Curve for all specimens

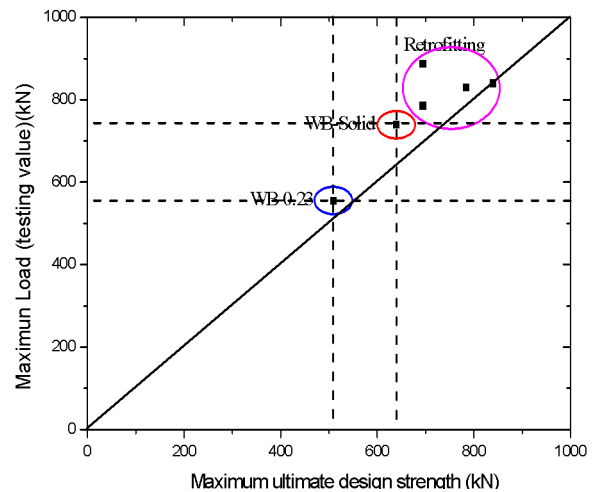


Figure 11. Maximum ultimate design load vs Maximum measured load

4. SUMMARY

In this research, wall specimens with openings were experimented in order to find out structural capacity of damaged wall and retrofitted wall. Test results this study are summarized below:

- 1) In the case of WB-0.23 which was damaged by installing an opening, ultimate strength of WB-0.23 decreased by 25% compared to that of WB-Solid. This was the result of loss of bond strength of horizontal reinforcement due to cutting of reinforcing bars and reduction of effective concrete area to transfer shear.
- 2) All specimens with openings initially showed flexural cracks because of stress concentration at the edge of the walls, and the cracks developed as shear cracks as the load increased.

3) Failure was caused predominantly by shear rather than flexure in all six wall specimens. For WB-CFS failure occurred by yielding of the sheets rather than debonding. However, debonding of the steel plate was the main cause of the failure of WB-St. Plate. In order to improve retrofitting effect for wall, CFS needed to be bonded to all wall surfaces by confining the wall. Steel plates were attached by anchoring steel plates to the wall surface.

4) For the strengthened specimens, partial failure occurred at the interface between wall and retrofitting material before the diagonal shear failure. However, Interface crack in WB-ECC propagated toward the wall, while interface crack in WB-MDF developed within the interface, since ECC material attached better on the wall face than MDF material.

5) Strength of the retrofitted specimens (Average of 836kN) was 12% higher on the average than that of WB-Solid. The stiffness reduction rate of the strengthened specimens, after the point of yielding of WB-Solid, was lower than WB-Solid. This is based on ineffective stress distribution to reinforcement. Although, retrofitted specimens showed higher value of peak load, energy dissipation capacity was lower than solid specimen. Therefore, energy dissipation capacity is the most important parameter for retrofitting of wall.

ACKNOWLEDGEMENT

This research was supported by a grant (07UrbanRenaissanceA03) from High-Tech Urban Development Program funded by the Ministry of Construction & Transportation of Korean Government and supported by the Korea Science and Engineering Foundation (KOSEF) funded by the Ministry of Education, Science and Technology (MEST) (No. R01-2008-000-11381-0) and the CCTRD of MOCT (grant C105A1050001-05A0505-00210).

REFERENCE

A.E., Naaman(2002): Toughness, Ductility, Surface Energy and Deflection-Hardening of FRC Composites, Proc. of JCI International Workshop on DFRCC, Oct., pp.33~57.

J. I. Daniel, K. N. Shiu, W. G. Corley F: Openings in Earthquake-Resistant Structural Walls, Journal of Structure Eng., ASCE, June 1, 1997, pp.1660-1675.

Paulay, T. and Priestley, M. J. N., "Seismic Design of Reinforced Concrete and Masonry Building," John Wiley & Sons Inc. 1992, pp.362 ~ 389

H. D. Yun, C. S. Choi, 2005. "Shear Strength and deformability of R/C Framed Shear Walls with Opening", Journal of the Architectural Institute of Korea, Structure & Construction, vol. 21, No.3, Mar. pp 11-18.

青山博之, "鉄筋コンクリート造開口耐震壁の補強設計法に関する研究", 東京大学青山研究室, 1991.

小野正行, "鉄筋コンクリート造有開口耐震壁の弾塑性性状に関する研究", 近畿大 博士学位論文, 2000.

Taylor, C. P., and Wallace, J. W., "Design of Slender Reinforced Concrete Walls with Openings" Report No. CU/CEE-95/13, Dept. of Civil and Environmental Eng'g, Clarkson Uni., Posdam, New York, 1995.

J. I. Daniel., K. N. Shiu., and W. G. Corle., "Openings in Earthquake-Resistant Structure Walls" Journal of Structural Engineering, Vol, 112, No.7, July, 1986, pp. 1660-1676.

ACI Committee 318, "Building Code Requirements for Structural Concrete (ACI 318-02) and Commentary (ACI 318 R-02)", American Concrete Institute, Michigan., 2002.

Darwin, D, and Nmai, C.K, "Energy Dissipation in RC Beams under Cyclic Load", Journal of Structural Div,

ASCE, Vol. 112, No.8, Aug 1986, pp. 1829-1846.

Luce, R., Individual Choice Behavior, John Wiley & Sons, 1959.

Tanabashi, R., "Experimental Investigation of the Decrease of Shear Resistance by the Opening in Wall," (Japanese), IJA, Apr., 1934, pp. 320-327.

Matsui, G., and Ogawa, T., "Study on Methods of Arranging Openings in Box Frame Type Construction and shearing Stress Distribution," Transactions of the Architectural Institute of Japan, No. 286, Dec., 1979, p.37-43.

Seya, Y., and Matsui, G., "Study of Stress and Displacement of Shear Wall with Opening," Transactions of the Architectural Institute of Japan, No. 286, Dec., 1979, pp.45-53.

H. D. Yun, C. S. Choi., 2003. "Shear Strength of High Strength Concrete Shear Walls", Journal of the Architectural Institute of Korea, Structure & Construction, Vol. 19, No. 5, May. pp. 53-60.

H. D. Yun, S. W. Kim, W. S. Park, H. J. Kim, C. S. Choi, G. B. Choi., 2005. "Structural Performance of Partial Cutting Rectangular R/C Shear Walls to form Opening", Journal of the Architectural Institute of Korea, Structure & Construction, vol. 21, No. 6, Jun. pp. 11-18.